ELSEVIER

Thermochimica Acta 266 (1995) 79–95

thermochimica acta

A glass transition due to freezing-in of positional disorder of mobile silver ions in the glassy state of the $AgBr–AgPO_3$ system ☆

Minoru Hanaya, Tomoyasu Okubayashi, Toshio Sakurai, Masaharu Oguni *

Department of Chemistry, Faculty of Science, Tokyo Institute of Technology, Ookayama, Meguro-ku, Tokyo 152, Japan

Abstract

Heat capacities and a.c. conductivities of $(AgBr)_x(AgPO_3)_{1-x}$ fast ion conducting glasses were measured in the temperature range 13–300 K, and in the temperature and frequency ranges 110–360 K and 10 Hz–1 MHz, respectively. β-Glass transitions due to the freezing-in of the rearrangement motion of Ag^+ ions were found by adiabatic calorimetry of the glasses with $x = 0.45$ and 0.55 in the liquid-nitrogen temperature region. Conductometry was applied to detect the same mode of Ag^+-ion motion as revealed by calorimetry. It is deduced that the positional order/disorder process of Ag^+ ions is essential to fast ionic conduction in the glasses and that the AgBr aggregates formed at high AgBr composition mainly contribute to the superionic conductivity of the glasses. On consideration of the energetic parameters concerning the rearrangement of Ag^+ ions, it is concluded that the AgBr aggregates have some amorphous structure that depends on the development of the aggregate region, as in the case of AgI-based fast ion conducting glasses, so that the fast Ag^+-ionic conduction can be realized in spite of the absence of a fast-ion-conducting crystalline phase in AgBr.

Keywords: Fast ion conduction; Glass transition; Heat capacity; Silver ion

* Corresponding author.

☆ Dedicated to Hiroshi Suga on the Occasion of his 65th Birthday.

SSDI 0040-6031(95)02446-8

1. Introduction

High-precision adiabatic calorimetry is now indispensable in the field of the physics and chemistry of condensed matter. H. Suga, together with coworkers, has made important contributions to the development of this calorimetry [1, 2], and has acted as a pioneer in showing that the close investigation of a glass transition by this method is useful for elucidation of both the static and kinetic energetics concerning the relevant configurational degrees of freedom of the glass transition [2, 3]. While elucidation of the properties of fast ionic conductors has not been a particular theme of his extensive work, it is not an exception in his line. Indeed, we have recently discovered β-glass transitions due to freezing-in of the rearrangement of conductive Ag^+ ions in typical fast ion conducting (FIC) $(AgI)_x(AgPO_3)_{1-x}$ glasses by precise heat-capacity measurements using an adiabatic calorimeter [4, 5]. From the analyses of the transition, the parameters representing the energetic environment around the conductive Ag^+ ions, namely the activation energy for the diffusional motion of conductive Ag^+ ions and the energy difference between the two lowest-energy sites accessible to each Ag^+ ion, have been derived and found to change continuously with AgI composition.

Ag^+-containing FIC glasses, especially AgI-based glasses, have been extensively investigated due to their high ionic conductivity of $\sim 10^{-2}$ S cm^{-1} and to interest in the mechanism and structure concerning fast ionic conduction [6–9]. The high ionic conductivity of AgI-based glasses has often been discussed in relation to the presence and structure of the well-known FIC crystalline phase, α-AgI. Meanwhile, the above calorimetric results have been reasonably well understood by considering that the AgI aggregate region naturally formed at high AgI compositions mainly contributes to the high ionic conductivity and, as a consequence, the "amorphous AgI aggregate" model has been proposed for the structure of the Ag^+ conductive region which changes with increasing AgI composition [5].

AgBr-based glasses have also been reported to exhibit considerably high ionic conductivities of $\sim 10^{-3}$ S cm^{-1}, and the conductivity is considered to derive from the AgBr component even though AgBr has no FIC crystalline phase [10–13]. This high ionic conductivity has been explained from the results of Raman and neutron-scattering experiments, as being due to the presence of $AgBr_4$ units of ordered structure, as in α-AgI, formed and dispersed in the glass matrix [14–16]. However, the structure and ionic conduction mechanism of these glasses are still under debate [17] and an unequivocal explanation of their conduction behavior is desired.

Precise calorimetry is expected to yield useful information also for AgBr-based glasses, and a comparison of the results with those of the $AgI–AgPO_3$ glass system should elucidate the overall structure and ionic conduction mechanism in these types of FIC glasses. Therefore, we used precise calorimetry and a.c. conductometry to examine a typical AgBr-based glass of $(AgBr)_x(AgPO_3)_{1-x}$ composition, and observed the glass transitions due to the freezing-in of the rearrangement of Ag^+ ions, as in the case of $(AgI)_x(AgPO_3)_{1-x}$ glasses. A quantitative knowledge of the energetic environment around the conductive Ag^+ ions and its dependence on the AgBr composition is derived from the results, and the structure of the ion-conductive region in the glasses is discussed based on this knowledge.

2. Experimental

$(AgBr)_x(AgPO_3)_{1-x}$ glasses were synthesized in low-light conditions from raw materials of reagent grade, namely AgBr, $AgNO_3$ and $NH_4H_2PO_4$, using the following procedure. The raw materials were weighed to the desired composition, mixed and ground in a mortar. The mixture was slowly heated up to 873 K and the red melt was quenched to room temperature by being pressed between a pair of stainless-steel plates. The cooling rate in this technique was estimated to be 10^2–10^3 K s^{-1}. For the $(AgBr)_x(AgPO_3)_{1-x}$ sample with the high AgBr composition of $x > 0.5$, a twin-roller quenching method was applied to yield a higher cooling rate, in which the melt was poured between the rotating twin rollers (3000 r.p.m.) at room temperature. The cooling rate by this method was estimated to be $\sim 10^5$ K s^{-1} [18]. Powder X-ray diffraction measurements were carried out using Cu Kα radiation, to confirm the successful preparation of glass samples containing no crystallites and to determine the glass-forming composition region.

Heat capacities of the glasses were measured in the temperature region between 13 and 300 K using an adiabatic calorimeter, as described previously [19]. A Pt resistance thermometer was used with calibration based on the ITS-90 [20]. The imprecision of the heat capacity was estimated to be ± 0.06% over the whole temperature range and within ± 0.03% in the liquid-nitrogen temperature region, and the inaccuracy was assessed to be within ± 0.3% from the results of the heat capacity measurements for benzoic acid as a standard material [19]. The sample used for the heat capacity measurements, which was in rather coarse flakes, was loaded in a calorimeter cell under an atmosphere of helium gas and the cell was sealed vacuum-tight with indium wire. The masses of the samples used were 40.206 g (corresponding to 0.21471 mol) for $(AgBr)_{0.45}(AgPO_3)_{0.55}$, and 21.924 g (0.11702 mol) for $(AgBr)_{0.55}(AgPO_3)_{0.45}$ glass, respectively.

The real and imaginary parts of the complex impedance for the $(AgBr)_x(AgPO_3)_{1-x}$ ($0 \leq x \leq 0.6$) glasses were measured as functions of both temperature (110–360 K) and frequency (10 Hz–1 MHz) employing an NF Electronic Instruments 2340 LCZ meter. Electrodes were prepared by painting silver paste on both sides of the thin plate sample obtained in the above press-quenching procedure or the film sample obtained in the twin-roller quenching procedure; in the latter case, the sample with the electrodes was stiffened with an epoxy resin to prevent the sample from breaking during the measurement. The a.c. conductivity was analyzed according to the electric modulus M^* formalism which has been employed for analyzing a.c. response of fast ion conducting glasses [5, 21, 22].

3. Results

3.1. Glass-forming composition region

Fig. 1 shows the powder X-ray diffraction patterns of the quenched $(AgBr)_x(AgPO_3)_{1-x}$ samples with relatively high AgBr compositions of $x \geq 0.50$. The

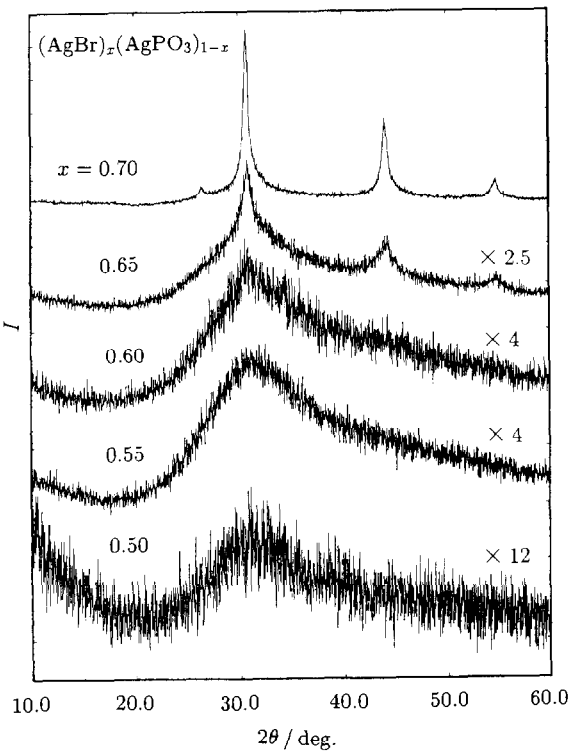

Fig. 1. Powder X-ray diffraction patterns of $(AgBr)_x(AgPO_3)_{1-x}$ at room temperature.

quenched samples with $x \leq 0.60$ exhibited only halo patterns characteristic of glassy states, and were confirmed to be glasses containing no crystallites. The quenched samples with the lower AgBr composition of $0 \leq x < 0.50$ also exhibited halo patterns. However, the $x = 0.65$ and 0.70 samples displayed weak and strong peaks, respectively, attributable to AgBr crystallites. Therefore, the formation of glass in the $(AgBr)_x(AgPO_3)_{1-x}$ system using the quenching technique described above was possible up to $x = 0.60$; AgBr crystallites are found in glasses with higher AgBr compositions.

3.2. Calorimetric results

The obtained molar heat capacities of $(AgBr)_x(AgPO_3)_{1-x}$ ($x = 0.45$ and 0.55) are shown in Fig. 2 and listed in Tables 1 and 2, respectively. Although each of the heat capacity curves was apparently quite smooth, an anomalous temperature dependence of the spontaneous temperature drift rates was observed for both glasses in the liquid-nitrogen temperature region during the heat-capacity measurements.

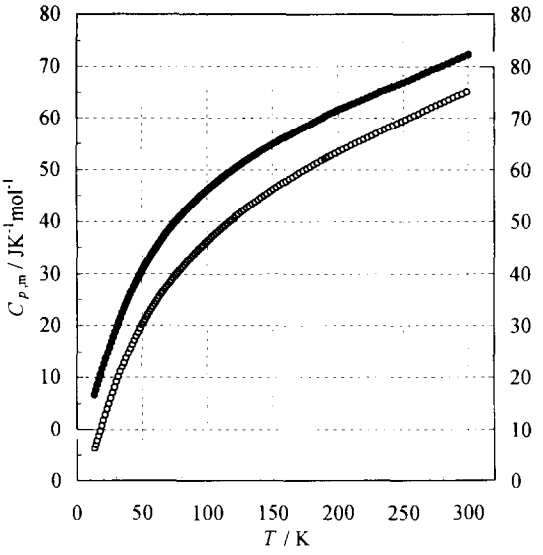

Fig. 2. Molar heat capacities of $(AgBr)_x(AgPO_3)_{1-x}$ glasses: ○, $x = 0.45$ glass; ●, $x = 0.55$ glass. The origin of the ordinate is shifted upward by 10 J K^{-1} mol^{-1} from $x = 0.45$ to $x = 0.55$ glasses.

Heat capacities were measured under adiabatic conditions by an intermittent heating method [5, 23] after samples were precooled down to low temperatures at some desired rate. Then spontaneous heat evolution or absorption due to enthalpy relaxation of the sample appeared as anomalous temperature drifts at positive or negative rates, respectively, of the calorimeter cell during the temperature-rating periods. Fig. 3 shows the temperature dependence of the spontaneous temperature drift rates observed during three separate series of heat capacity measurements of the $x = 0.55$ glass. Closed circles (corresponding to Series 1 in Table 2) represent the result for the sample precooled rapidly in the liquid-nitrogen temperature region at the approximate rate of 8 K min^{-1}. The sample exhibited an exothermic effect starting at about 65 K, showing its maximum at about 78 K, and changing to a relatively small endothermic effect at about 90 K. Open circles (Series 2) and open squares represent the results for samples precooled slowly at an approximate rate of 12 mK min^{-1}. The samples showed only an endothermic effect starting at about 70 K with a peak at about 84 K, and the drift rates returned to normal at about 97 K.

These exothermic and/or endothermic effects that change with the precooling rates are recognized as characteristic feature of a glass transition [3, 24], and definitely indicate the existence of a β-glass transition different from the α-glass transition expected above room temperature [13]. In this glass, the fast ionic conduction is considered to arise from the presence of Ag^+ ions with remarkably high mobility, and it is reasonable to assign the β-glass transition to the freezing-in of the rearrangement of the Ag^+ ions because the positions of the other ions in the glass are fixed at such low temperatures, much below the α-glass transition temperature.

Table 1
Molar heat capacities, $C_{p,m}$, of $(AgBr)_{0.45}(AgPO_3)_{0.55}$ glass

Series 1 (rapidly cooled at 8 K min^{-1})				Series 2 (slowly cooled at 11 mK min^{-1})					
T_{av}/K	$C_{p,m}$/(J K^{-1} mol^{-1})	T_{av}/K	$C_{p,m}$/(J K^{-1} mol^{-1})	T_{av}/K	$C_{p,m}$/(J K^{-1} mol^{-1})	T_{av}/K	$C_{p,m}$/(J K^{-1} mol^{-1})	T_{av}/K	$C_{p,m}$/(J K^{-1} mol^{-1})
13.56	6.171	63.44	35.53	66.33	36.56	126.13	51.74	219.71	65.75
14.54	6.964	64.75	36.02	67.70	37.04	128.24	52.14	222.89	66.15
15.59	7.811	66.08	36.48	69.09	37.51	130.38	52.55	226.08	66.51
16.68	8.694	67.41	36.95	70.50	37.98	132.55	52.93	229.29	66.90
17.90	9.668	68.77	37.41	71.91	38.44	134.75	53.33	232.51	67.34
19.20	10.70	70.13	37.86	73.34	38.90	136.99	53.74	235.73	67.69
20.46	11.70	71.51	38.32	74.78	39.34	139.25	54.14	238.97	68.08
21.81	12.75	72.91	38.76	76.23	39.79	141.54	54.55	242.22	68.47
23.24	13.84	74.31	39.21	77.69	40.22	143.86	54.95	245.47	68.87
24.67	14.91	75.73	39.63	79.17	40.67	146.20	55.34	248.74	69.24
26.13	15.98	77.17	40.06	80.66	41.10	148.58	55.74	252.02	69.61
27.60	17.03	78.61	40.49	82.16	41.52	150.99	56.15	255.31	70.02
29.10	18.07	80.07	40.93	83.68	41.95	153.43	56.54	258.61	70.41
30.60	19.09	81.55	41.34	85.20	42.36	155.89	56.96	261.92	70.80
32.10	20.08	83.03	41.76	86.74	42.78	158.39	57.35	265.24	71.22
33.61	21.05	84.53	42.16	88.29	43.20	160.91	57.73	268.57	71.60
35.13	22.00	86.04	42.59	89.86	43.61	163.46	58.12	271.92	71.99
36.64	22.92	87.57	42.99	91.43	44.01	166.04	58.52	275.27	72.36
38.15	23.81	89.11	43.40	93.02	44.44	168.65	58.91	278.63	72.75
39.67	24.68	90.66	43.81	94.62	44.83	171.29	59.35	282.00	73.11
41.18	25.52	92.22	44.21	96.24	45.23	173.95	59.75	285.38	73.52
42.69	26.35	93.80	44.61	97.86	45.62	176.64	60.09	288.77	73.91
44.20	27.14	95.39	45.00	99.51	46.02	179.36	60.48	292.17	74.28
45.72	27.92	96.99	45.40	101.16	46.40	182.11	60.87	295.59	74.61
47.23	28.68	98.60	45.78	102.83	46.79	184.88	61.28	299.01	75.00
48.75	29.41	100.23	46.17	104.50	47.17	187.68	61.68		
50.27	30.13	101.87	46.56	106.20	47.54	190.50	62.07		
51.29	30.58	103.53	46.95	107.90	47.92	192.40	62.34		
52.42	31.09	105.19	47.31	109.62	48.29	193.38	62.46		
53.57	31.59	106.87	47.70	111.35	48.67	195.34	62.73		
54.74	32.09	108.57	48.07	113.10	49.02	198.26	63.11		
55.93	32.61	110.27	48.43	114.86	49.39	201.23	63.47		
57.14	33.10	111.99	48.79	116.63	49.75	204.22	63.85		
58.37	33.59	113.73	49.17	118.42	50.12	207.25	64.23		
59.61	34.09	115.47	49.52	120.79	50.60	210.31	64.62		
60.87	34.57	117.23	49.89	122.01	50.94	213.41	65.00		
62.15	35.06	119.01	50.23	124.06	51.34	216.54	65.37		

The observed enthalpy relaxation effect during the β-glass transition was unfortunately so small that the relaxation time at each temperature in the transition region could not be estimated experimentally from the rate of enthalpy relaxation. However, in many cases of glass transitions, samples precooled at a low rate of about 10 mK

Table 2
Molar heat capacities, $C_{p,m}$, of $(AgBr)_{0.55}(AgPO_3)_{0.45}$ glass

Series 1 (rapidly cooled at 8 K min^{-1})				Series 2 (slowly cooled at 12 mK min^{-1})					
T_{av}/K	$C_{p,m}$/(J K^{-1} mol^{-1})	T_{av}/K	$C_{p,m}$/(J K^{-1} mol^{-1})	T_{av}/K	$C_{p,m}$/(J K^{-1} mol^{-1})	T_{av}/K	$C_{p,m}$/(J K^{-1} mol^{-1})	T_{av}/K	$C_{p,m}$/(J K^{-1} mol^{-1})
13.62	6.604	60.13	34.66	50.58	30.71	99.43	45.85	185.58	59.61
14.76	7.550	61.26	35.08	51.45	31.09	100.97	46.17	188.48	59.96
15.96	8.527	62.40	35.50	52.45	31.53	102.51	46.51	190.26	60.35
17.16	9.514	63.56	35.91	53.48	31.98	104.07	46.85	193.29	60.72
18.42	10.52	64.74	36.34	54.53	32.43	105.64	47.16	196.36	61.05
19.75	11.59	65.92	36.73	55.59	32.87	107.22	47.48	199.46	61.46
21.07	12.63	67.12	37.14	56.67	33.32	108.80	47.79	202.60	61.76
22.41	13.68	68.32	37.54	57.76	33.74	110.40	48.11	205.77	62.09
23.81	14.74	69.54	37.95	58.87	34.18	112.01	48.42	205.77	62.09
25.21	15.79	70.77	38.34	60.00	34.62	113.63	48.74	208.98	62.43
26.61	16.80	72.01	38.72	61.13	35.03	115.26	49.04	212.23	62.77
27.99	17.79	73.27	39.12	62.29	35.47	116.90	49.34	215.51	63.11
29.37	18.75	74.53	39.49	63.45	35.87	119.84	49.87	218.83	63.44
30.74	19.67	75.81	39.86	64.63	36.29	122.01	50.26	222.19	63.80
32.10	20.57	77.09	40.23	65.81	36.70	124.21	50.66	225.58	64.15
33.44	21.43	78.39	40.60	67.01	37.12	126.45	51.04	229.00	64.52
34.78	22.27	79.70	40.98	68.23	37.51	128.71	51.43	232.47	64.99
36.11	23.09	81.01	41.32	69.45	37.92	130.99	51.80	235.96	65.31
37.42	23.88	82.34	41.67	70.68	38.32	133.31	52.19	239.49	65.66
38.73	24.63	83.68	42.04	71.93	38.70	135.66	52.55	243.06	66.05
40.03	25.37	85.03	42.39	73.24	39.10	138.03	52.94	246.66	66.42
41.32	26.08	86.39	42.74	74.63	39.53	140.43	53.33	250.30	66.80
42.61	26.78	87.76	43.09	76.03	39.94	142.86	53.70	253.97	67.18
43.89	27.45	89.14	43.43	77.43	40.35	145.32	54.08	257.67	67.61
45.17	28.11	90.53	43.78	78.84	40.76	147.81	54.46	261.41	68.03
46.44	28.75	91.94	44.11	80.26	41.18	150.33	54.83	265.18	68.48
47.71	29.36	93.35	44.45	81.68	41.54	152.87	55.15	268.98	68.87
48.98	29.97	94.77	44.80	83.12	41.94	155.44	55.54	272.82	69.36
50.24	30.56	96.21	45.11	84.56	42.31	158.04	55.92	276.69	69.68
50.78	30.78	97.65	45.44	86.00	42.71	160.67	56.29	280.59	70.07
51.63	31.17	99.11	45.76	87.46	43.06	163.32	56.66	284.52	70.46
52.63	31.61	100.57	46.09	88.93	43.43	166.01	57.02	288.49	70.93
53.65	32.04	102.05	46.41	90.40	43.80	168.72	57.39	292.49	71.37
54.69	32.50	103.54	46.74	91.88	44.13	171.46	57.75	296.52	71.76
55.74	32.93	105.04	47.02	93.37	44.49	174.23	58.15	300.59	72.19
56.82	33.38	106.55	47.35	94.87	44.83	177.02	58.47		
57.90	33.81	108.07	47.65	96.38	45.17	179.85	58.83		
59.01	34.22	109.61	47.96	97.90	45.50	182.70	59.22		

min^{-1} in the transition region have been observed to exhibit, in the following intermittent heating process of the heat capacity measurements with a temperature-rating period of about 10 min, an endothermic peak in the spontaneous temperature drift rate curve at the temperature where the relaxation time is about 1 ks [19, 24].

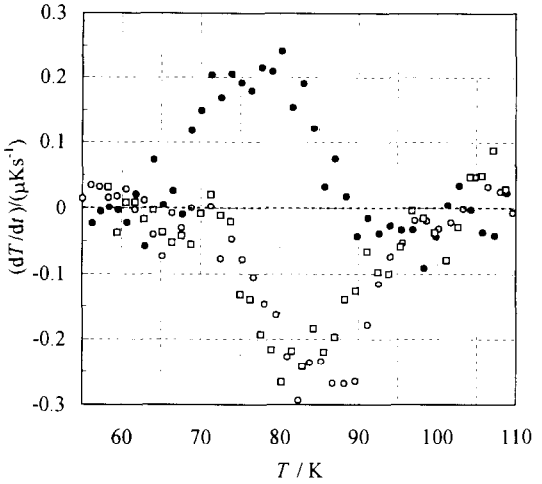

Fig. 3. Spontaneous temperature drift rates observed during three separate series of heat-capacity measurements of $(AgBr)_{0.55}(AgPO_3)_{0.45}$ glass in the liquid-nitrogen temperature region: ●, rapidly precooled sample at an approximate cooling rate of 8 K min^{-1}; ○, □, slowly precooled sample at an approximate cooling rate of 12 mK min^{-1}.

According to this empirical law, the β-glass transition temperature, T_g, at which the relaxation time became 1 ks was found to be 84 ± 1 K for the $x = 0.55$ glass.

For a clear assessment of the very small heat capacity jump associated with the β-glass transition, the heat-capacity data were treated as follows. First the observed heat capacities were converted to the apparent partial molar quantities of AgBr by subtracting the heat capacity contribution from the glassy $AgPO_3$ portion [4, 5]; then a smooth curve was obtained. The smooth curve was determined somewhat arbitrarily by fitting to the obtained partial molar AgBr heat capacity data below 57 K, a function represented as the sum of the Debye and Einstein functions for each of three vibrational degrees of freedom and a $C_p - C_v$ correction term of AC_p^2T. The excess heat capacities over the smooth curve around the β-glass transition region are shown in Fig. 4, which clearly indicates the heat capacity jump associated with the transition. Open circles (corresponding to Series 2 in Table 2) and squares in the figure are the results of the slowly precooled sample, and closed circles (Series 1) are those of the rapidly precooled sample, respectively. In the slowly precooled sample, overshooting effects were seen in the glass transition temperature region because the heat capacities were evaluated so as to include the contribution due to the endothermic enthalpy relaxation associated with the glass transition during the measurements. However, below T_g the rapidly precooled sample showed only the heat capacities due to the vibrational degrees of freedom of the non-equilibrium glass, because the heat capacities were evaluated to exclude the contribution from the exothermic enthalpy relaxation by recognizing the exothermic temperature drift as being attributed to the heat influx from the surroundings of the cell. The two dashed lines in the lower and higher temperature regions represent the

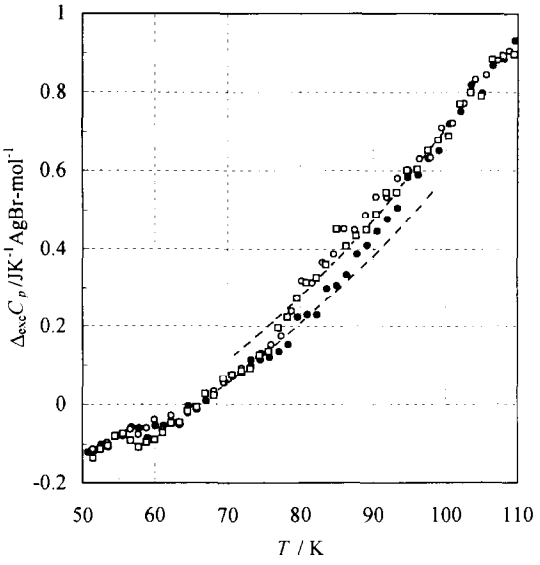

Fig. 4. Temperature dependence of excess heat capacities around the β-glass transition temperature in $(AgBr)_{0.55}(AgPO_3)_{0.45}$ glass: ●, rapidly precooled sample at an approximate cooling rate of 8 K min^{-1}; ○,□, slowly precooled sample at an approximate cooling rate of 12 mK min^{-1}. The values were derived as referred to a smooth curve somewhat arbitrarily drawn for the apparent partial molar heat capacities of AgBr (see text for detail).

assessed heat capacity curves in the frozen-in and in the equilibrium states, respectively, with respect to the configurational degrees of freedom of Ag^+ ions relevant to the β-glass transition. From the difference between the two dashed lines, the heat-capacity jump at the β-glass transition temperature, 84 K, was evaluated to be 0.06 ± 0.02 J K^{-1} (AgBr mol)$^{-1}$ and thus 0.03 ± 0.01 J K^{-1} mol^{-1} for $(AgBr)_{0.55}(AgPO_3)_{0.45}$ glass, which corresponded to 0.07% of the molar heat capacity of the glass at this temperature.

Similar calorimetric behavior was also observed in the $x = 0.45$ glass. The temperature dependence of the spontaneous temperature drift rates observed during the series of heat capacity measurements and the excess part of the apparent partial molar heat capacities of AgBr in the glass, evaluated as in the above case of $x = 0.55$ glass, are shown in Fig. 5. The β-glass transition temperature was determined as 95 ± 1 K from the endothermic peak in the spontaneous temperature drift rate curve (Fig. 5a), and the heat capacity jump associated with the glass transition was assessed from the difference between the two dashed lines (Fig. 5b) as 0.04 ± 0.02 J K^{-1}(AgBr-mol)$^{-1}$ and, thus, 0.02 ± 0.01 J K^{-1} mol^{-1} for $x = 0.45$ glass at the glass transition temperature. The jump corresponded to 0.04% of the molar heat capacity of the glass at the glass transition temperature as a magnitude of the just distinguishable limit, in view of the imprecision ($\pm 0.03\%$) of calorimetry in the relevant temperature range.

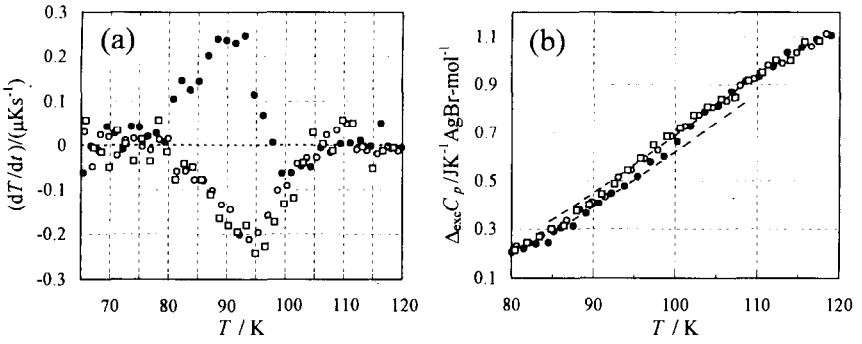

Fig. 5. (a) Spontaneous temperature drift rates observed during three separate series of heat capacity measurements of $(AgBr)_{0.45}(AgPO_3)_{0.55}$ glass in the liquid-nitrogen temperature region. (b) Temperature dependence of excess heat capacities around the β-glass transition temperature: ●, rapidly precooled sample at an approximate cooling rate of 8 K min^{-1}; ○,□, slowly precooled sample at an approximate cooling rate of 11 mK min^{-1}. In (b), the values were derived using the same procedure as in the case of $(AgBr)_{0.55}(AgPO_3)_{0.45}$ glass.

3.3. A.c. conductivity behavior

The imaginary component of the complex electrical modulus, M'', measured at several different temperatures for the $x = 0.40$ glass is plotted against the logarithm of frequency in Fig. 6. This plot exhibits features typical of M'' spectra of all the glasses presently studied: the frequency of the M'' peak, $f_{M''}$, was observed to increase with

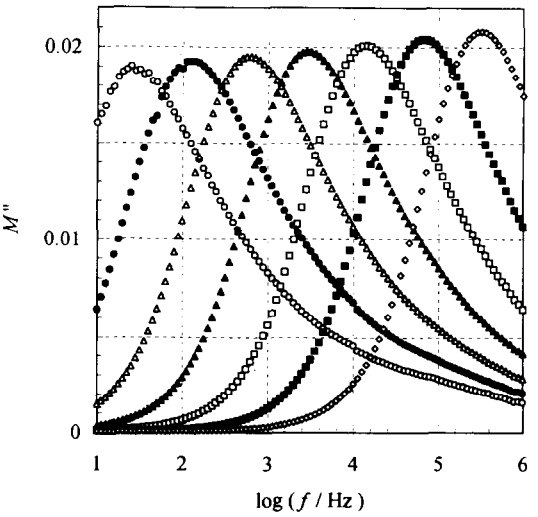

Fig. 6. Isothermal M'' spectra for $(AgBr)_{0.40}(AgPO_3)_{0.60}$ glass at different temperatures: ○, 147 K; ●, 156 K; Δ, 167 K; ▲, 179 K; □, 192 K; ■, 208 K; ◇, 227 K.

increasing temperature, while the height changed slightly and the frequency width at half the height of the peak remained almost unchanged with temperature. Since M'' reflects the dispersion of the rates of response to the electric field in the glasses, $f_{M''}$ is considered to represent the mean frequency of the fluctuational motion of conductive Ag^+ ions in the glass at the specific temperature, and thus the relaxation time, $\tau(T)$, associated with the diffusional motion of conductive Ag^+ ions at the temperature was derived from the frequency, $f_{M''}(T)$, according to the relation $\tau(T) = 1/(2\pi f_{M''}(T))$.

Fig. 7 shows Arrhenius plots of the derived conductometric relaxation times for the presently studied $(AgBr)_x(AgPO_3)_{1-x}$ glasses together with the calorimetric relaxation times for the $x = 0.45$ and 0.55 glasses. Solid lines in the figure represent the results of the least-squares fitting of a straight line to the conductometric data for each glass, respectively. All the relaxation times are well fitted by the respective straight lines for the glasses, and the intercept of $\sim 10^{-14}$ s is within an appropriate order of magnitude in view of the frequency of translational vibration of Ag^+ ions. The good fit of the relaxation times to a straight line signifies that the potential curve for the positional rearrangement of the Ag^+ ions is virtually unchanged in the temperature range presently studied below the α-glass transition temperature, and thus the arrangement of ions other than the conductive Ag^+ ions is considered to be basically fixed at the α-glass transition temperature.

Moreover, the calorimetric results fall well on the corresponding extrapolated lines. This signifies that the relaxation phenomena observed by a.c. conductometry and calorimetry have the same origin, the motions of Ag^+ ions, and the β-glass transition

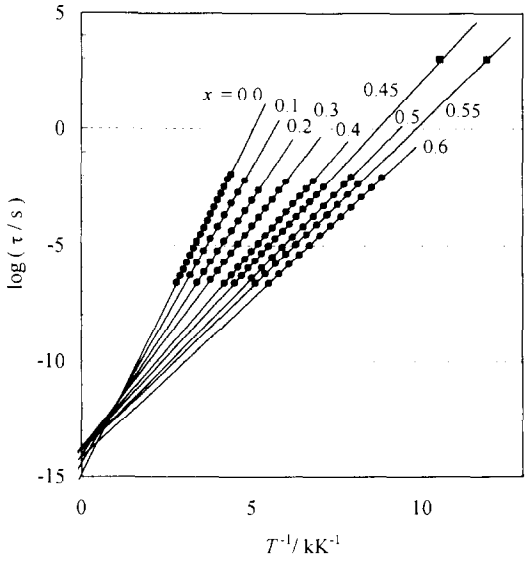

Fig. 7. Arrhenius plots of the relaxation times associated with the diffusional motion of Ag^+ ions in $(AgBr)_x(AgPO_3)_{1-x}$ glasses. Solid circles and squares are the results obtained by a.c. conductometry and calorimetry, respectively. Solid lines were derived from least-squares fitting of a straight line to the a.c. conductometric data for each glass.

observed by calorimetry is clearly indicated to be due to freezing-in of the rearrangement of conductive Ag^+ ions.

Activation energies for the diffusional motion of conductive Ag^+ ions in these glasses were calculated from the slopes of the lines, and the dependence of the activation energy on AgBr composition, x, is shown in Fig. 8 together with the result for the $AgI–AgPO_3$ glass system for comparison [25].

4. Discussion

$(AgBr)_x(AgPO_3)_{1-x}$ glasses with the relatively high AgBr compositions of $x = 0.45$ and 0.55 show the β-glass transitions which are reasonably well understood as being attributed to the freezing-in of the positional rearrangement of conductive Ag^+ ions. Calorimetry is sensitive only to the configurational (positional) disorder of the Ag^+ ions, while conductometry detects the diffusional motion of the ions under an electric field. This indicates that the fast ionic conductivity of the glasses is connected with the presence of positional disorder of the Ag^+ ions. Meanwhile, as in the case of $AgI–AgPO_3$ glasses, the activation energy for the diffusional motion of conductive Ag^+ ions decreases continuously with AgBr composition as shown in Fig. 8, and the heat capacity jump associated with the transition increases with the increase in AgBr composition as shown in Fig. 9. These signify that the presence of conductive Ag^+ ions, and thus fast ionic conductivity, in the glasses under study derive from the AgBr component, although the bulk AgBr has no fast ionic conducting phase in the

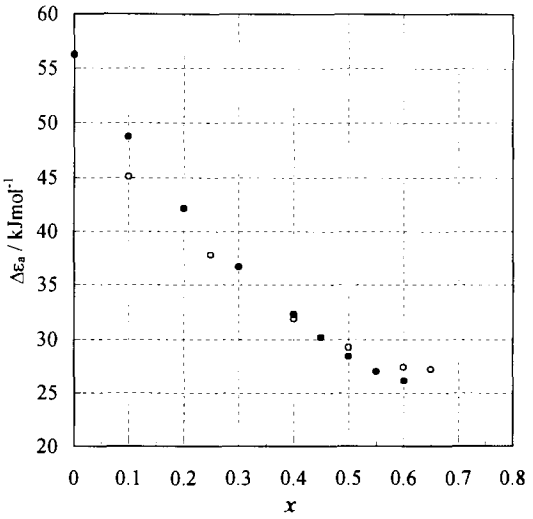

Fig. 8. AgBr and AgI composition dependence of the activation energies, $\Delta\varepsilon_a$, for the rearrangement of conductive Ag^+ ions derived from the a.c. conductometry: ●, $(AgBr)_x(AgPO_3)_{1-x}$ glasses; ○, $(AgI)_x(AgPO_3)_{1-x}$ glasses [25].

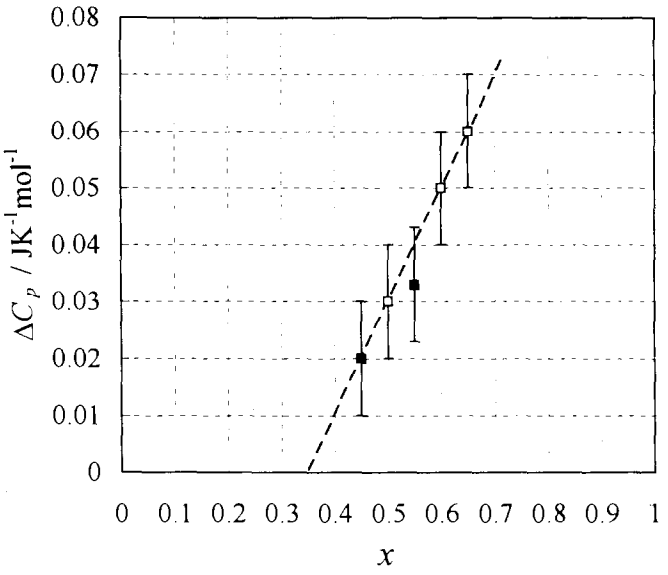

Fig. 9. AgBr and AgI composition dependence of the heat capacity jump in the β-glass transition associated with rearrangement of Ag^+ ions for $(AgX)_x(AgPO_3)_{1-x}$ (X is Br, I) glasses: ■, $(AgBr)_x(AgPO_3)_{1-x}$ glasses; □, $(AgI)_x(AgPO_3)_{1-x}$ glasses [5].

crystalline state. Moreover, the distinct observation of the β-glass transition means that appreciable amounts of Ag^+ ions are located in almost the same energetic environments; this would be otherwise impossible in view of the nature of calorimetry. Fig. 10 shows a schematic two-dimensional representation of the glass structure of $(AgBr)_x(AgPO_3)_{1-x}$ glass at moderately high AgBr composition. The AgBr aggregate region containing only Ag^+ and Br^- ions is naturally formed in the glass as the AgBr composition becomes high. The reason is that $AgPO_3$ has a chain structure and cannot be dispersed so much in the glass. The above AgBr composition dependence of the calorimetric and a.c. conductometric properties of the glasses indicate that the Ag^+ ions included in the AgBr aggregate region, namely the Ag^+ ions surrounded only by Br^- ions, mainly contribute to the fast ionic conduction of the glass, and are located more or less in the same energetic environments as are responsible for the β-glass transition.

The AgBr aggregate region, as a matter of course, is absent at low AgBr contents, appears at some composition of x_c, increases with increasing AgBr composition in proportion to $(x - x_c)$ [5], and finally undergoes the inevitable crystallization of AgBr above $x = 0.65$ as shown in the powder X-ray diffraction results. The AgBr composition dependence of the heat capacity jump, ΔC_p, at the β-glass transition temperature in the glasses with $x = 0.45$ and 0.55 is consistent with this view, as shown in Fig. 9 together with that in the AgI–$AgPO_3$ glass system [5]. The ΔC_p increases with x in the same way as in the AgI–$AgPO_3$ glass system. A linear relation can be assumed between the heat capacity jump and the AgBr mole fraction according to the above view, and a reason-

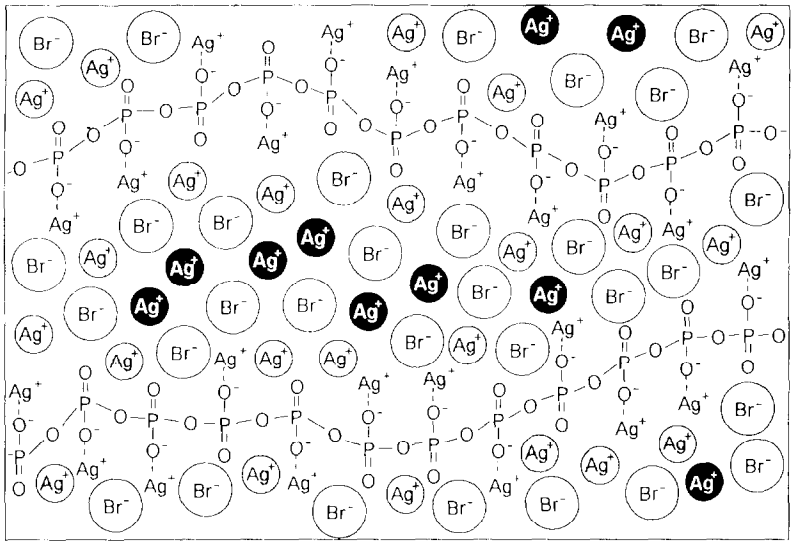

Fig. 10. Schematic two-dimensional representation of glass structure in the $(AgBr)_x(AgPO_3)_{1-x}$ glass at moderately high AgBr composition. Three types of Ag^+ ions are presented; --- Ag^+ ions are Ag^+ ions bonded with the non-bridging oxygen of PO_3^-, circled Ag^+ are those interacting with meta-phosphate units as well as Br^- ions, and solid circled Ag^+ are those surrounded by Br^- ions only.

ably straight dashed line is drawn in the figure. The amount of AgBr contributing to the β-glass transition in $(AgBr)_x(AgPO_3)_{1-x}$ can be expressed by the formula $(x - x_c)/(1 - x_c)$, as the mole fraction of $AgPO_3$ decreases with increasing x above x_c and then the proportionality constant is deduced to be $1/(1 - x_c)$. The value of x_c is estimated to be about 0.35 as the intercept of the dashed line to the abscissa, and applying this formula to the $x = 0.45$ and 0.55 glasses gives rise to an estimation of 0.15 and 0.31 mol, respectively, of AgBr contributing to the β-glass transition, and thus to the heat capacity jump at the transition for 1 mol of the glasses.

The glass transition observed by calorimetry is the freezing-in phenomenon of the configurational order/disorder process activated by the thermal energy kT. While the β-glass transition temperature reflects the activation energy $\Delta\varepsilon_a$ of the potential along the path of positional rearrangement of Ag^+ ions, as shown schematically in Fig. 11, the heat capacity jump associated with the glass transition includes information about the energy difference $\Delta\varepsilon$ between some neighboring lowest-energy sites for the Ag^+ ions. The heat capacity jump in the β-glass transition was very small. This indicates that only a small fraction of the relevant Ag^+ ions above estimated possess excited-in-energy positions. In such a situation, it is reasonable to assume that only a small fraction of the relevant Ag^+ ions take up the first excited state and contribute to the observed heat capacity jump as a macroscopic property. Thus, the two-level scheme was used here to derive information about the energetic circumstance for the accessible positions to each Ag^+ ion. According to the two-level scheme, the molar heat capacity

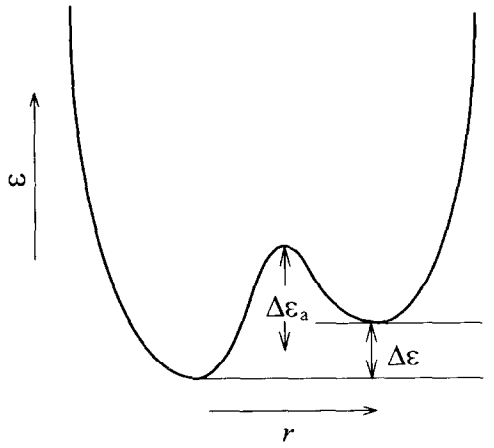

Fig. 11. Schematic potential diagram along the path of positional rearrangement of an Ag^+ ion. The abscissa, r, represents the position of an Ag^+ ion. $\Delta\varepsilon_a$ and $\Delta\varepsilon$ denote the potential barrier and the difference between the two lowest potential minima, respectively.

due to the Ag^+ ions can be expressed by the following equation with $\Delta\varepsilon$

$$C = R[(\Delta\varepsilon/RT)^2 \exp(\Delta\varepsilon/RT)/\{1 + \exp(\Delta\varepsilon/RT)\}^2]$$

The molar value C can be related to the magnitude of the observed heat capacity jump by $C = \Delta C_p/[(x - x_c)/(1 - x_c)]$, in which the denominator is the amount of AgBr contributing to the heat capacity jump as mentioned above. The differences between the lowest two potential minima for Ag^+ positions are estimated from the calculations to be 6.7 ± 0.7 and 6.1 ± 0.6 kJ mol^{-1} for $x = 0.45$ and 0.55 glasses, respectively.

The activation energy, $\Delta\varepsilon_a$, and the difference between the neighboring lowest two potential minima, $\Delta\varepsilon$, are listed in Table 3 together with the calorimetric results for the β-glass transition temperature, T_g, and the heat capacity jump at the glass transition temperature, ΔC_p. From the fact that $\Delta\varepsilon_a$ and $\Delta\varepsilon$ decrease with increasing AgBr composition, it is obvious that the structural feature of the AgBr aggregate dominating the fast ionic conduction of the glasses changes with AgBr composition. One may consider that the fast ionic conductivity of the $AgBr–AgPO_3$ glass system derives from AgBr clusters formed in the glass, with an ordered crystalline structure like α-AgI, and

Table 3
Calorimetric results for the β-glass transition and the energetic environment around the conductive Ag^+ ions

Glass sample	T_g/K	ΔC_p/(J K^{-1} mol^{-1})	$\Delta\varepsilon_a$/(kJ mol^{-1})	$\Delta\varepsilon$/(kJ mol^{-1})
$(AgBr)_{0.45}(AgPO_3)_{0.55}$	95±1	0.02±0.01	30.2±0.3	6.7±0.7
$(AgBr)_{0.55}(AgPO_3)_{0.45}$	84±1	0.03±0.01	27.0±0.2	6.1±0.6

from the percolation of Ag^+ ions through the clusters [14–16]. Such a crystalline form, even if it is unobtainable in the bulk AgBr, would be likely when the crystallite is composed of a small number of ions. If the AgBr aggregate was constructed of such AgBr clusters and only the number of the clusters increased with the AgBr composition without changing their microstructure, however, the energetic environment around the conductive Ag^+ ions would not change with AgBr composition. The AgBr composition dependence of Δc_a and Δc thus suggests that the AgBr aggregate has some amorphous structure depending on the degree of development of the AgBr aggregation region which is expected to grow in size with AgBr composition. The fast Ag^+-ionic conduction, which is unobtainable in the AgBr crystalline phase, is thought to occur in such an amorphous AgBr aggregate region which has, indeed, disordered structure with positional disorder of conductive Ag^+ ions. Therefore, the "amorphous AgI aggregate" model postulated for the structure of the AgI-based fast ion conducting glasses [5, 26] is also indicated as being applicable to the AgBr-based fast ion conducting glasses presently studied, and this implies some validity for the model of the structure of these kinds of fast ion conducting glass based not only on AgX (X is I, Br and Cl) but also on LiX and CuX.

It should be noted here that the activation energies in the $AgBr–AgPO_3$ glasses are not so different from those in $AgI–AgPO_3$ glasses at the same AgX composition, while the conductivity of the former is lower by almost one order than that of the latter at room temperature. Unfortunately, this discrepancy cannot be explained without more precise information about the energetic environment as well as the positional arrangement of ions around the conductive Ag^+ ions for both AgI- and AgBr-based fast ion conducting glasses. To gain an insight into this problem, calorimetric and conductometric studies of AgI–AgBr mixed glass systems are now in progress in our laboratory.

References

[1] H. Suga and S. Seki, Bull. Chem. Soc. Jpn., 38 (1965) 1000.
[2] H. Suga and S. Seki, J. Non-Cryst. Solids, 16 (1974) 171.
[3] H. Suga and S. Seki, Faraday Discuss., 69 (1980) 221.
[4] M. Nakayama, M. Hanaya and M. Oguni, Solid State Commun., 89 (1994) 403.
[5] M. Nakayama, M. Hanaya, A. Hatate and M. Oguni, J. Non-Cryst. Solids, 172–174 (1994) 1252.
[6] C.A. Angell, Ann. Rev. Phys. Chem., 43 (1992) 693.
[7] S.W. Martin, J. Am. Ceram. Soc., 74 (1991) 1767.
[8] T. Minami, J. Non-Cryst. Solids, 95/96 (1987) 107.
[9] M.D. Ingram, Phys. Chem. Glasses, 28 (1987) 215.
[10] T. Minami, T. Shimizu and M. Tanaka, Solid State Ionics, 9/10 (1983) 577.
[11] G. Robert, J.P. Malugani and A. Saida, Solid State Ionics, 3/4 (1981) 311.
[12] T. Minami and M. Tanaka, Rev. Chim. Miner., 16 (1979) 283.
[13] J.P. Malugani, A. Wasniewski, M. Doreau, G. Robert and A. Al Rikabi, Mater. Res. Bull., 13 (1978) 427.
[14] A.J. Dianoux, M. Tachez, R. Mercier and J.P. Malugani, J. Non-Cryst. Solids, 131–133 (1991) 973.
[15] C. Rousselot, M. Tachez, J.P. Malugani, R. Mercier and P. Chieux, Solid State Ionics, 44 (1991) 151.
[16] J.P. Malugani and R. Mercier, Solid State Ionics, 13 (1984) 293.
[17] A. Musinu, G. Paschina, G. Piccaluga and G. Pinna, Solid State Ionics, 34 (1989) 187.

[18] M. Hanaya, M. Nakayama, M. Oguni, M. Tatsumisago, T. Saito and T. Minami, Solid State Commun., 87 (1993) 585.
[19] H. Fujimori and M. Oguni, J. Phys. Chem. Solids, 54 (1993) 271.
[20] H. Preston-Thomas, Metrologia, 27 (1990) 3.
[21] M.B.M. Mangion and G.P. Johari, Phys. Chem. Glasses, 29 (1988) 225.
[22] M.C.R. Shastry and K.J. Rao, Solid State Ionics, 44 (1991) 187.
[23] E.F. Westrum, Jr., G.T. Furukawa and J.P. McCullough, in J.P. McCullough and D.W. Scott (Eds.), Experimental Thermodynamics, Vol. 1, Butterworths, London, 1968, p. 133.
[24] M. Oguni, T. Matsuo, H. Suga and S. Seki, Bull. Chem. Soc. Jpn., 50 (1977) 825.
[25] A. Hatate, M. Hanaya and M. Oguni, unpublished data.
[26] M. Hanaya, M. Nakayama, A. Hatate and M. Oguni, Phys. Rev. B, in press.